

AD-A190 603

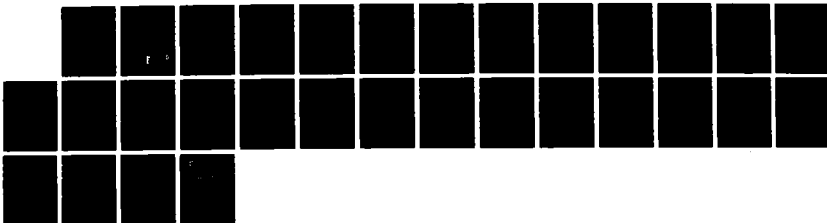
RETROREFLECTANCE OF WIRES AND CABLES AT 106 MICROMETERS
(U) CENTER FOR NIGHT VISION AND ELECTRO-OPTICS FORT
BELVOIR VA H SAVAN ET AL. JAN 88 ANSEL-NV-TR-0063

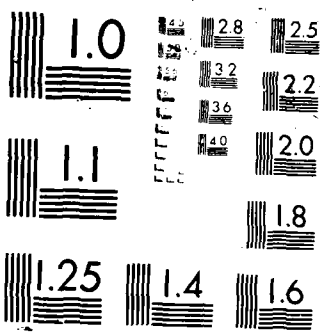
1/1

UNCLASSIFIED

F/G 17/9

NL





2

AD-A190 603

Center for Night Vision and Electro-Optics

AMSEL-NV-TR-0063

RETROREFLECTANCE OF WIRES AND CABLES AT 10.6 MICROMETERS

by
Mark Savan and Dallas N. Barr

January 1988

Approved for public release; distribution unlimited.



DTIC
ELECTE
MAR 1 1 1988
S D H

FORT BELVOIR, VIRGINIA 22060-5677

Unclassified

SECURITY CLASSIFICATION OF THIS PAGE

REPORT DOCUMENTATION PAGE

Form Approved OMB No. 0704-0188

1a. REPORT SECURITY CLASSIFICATION Unclassified		1b. RESTRICTIVE MARKINGS None		A190 608	
2a. SECURITY CLASSIFICATION AUTHORITY		3. DISTRIBUTION / AVAILABILITY OF REPORT Approved for public release; distribution unlimited.			
2b. DECLASSIFICATION / DOWNGRADING SCHEDULE		4. PERFORMING ORGANIZATION REPORT NUMBER(S) AMSEL-NV-TR-0063		5. MONITORING ORGANIZATION REPORT NUMBER(S)	
6a. NAME OF PERFORMING ORGANIZATION Center for Night Vision and Electro-Optics (CNVEO)		6b. OFFICE SYMBOL (if applicable) AMSEL-RD-NV-L	7a. NAME OF MONITORING ORGANIZATION		
6c. ADDRESS (City, State, and ZIP Code) Fort Belvoir, VA 22060-5677		7b. ADDRESS (City, State, and ZIP Code)			
8a. NAME OF FUNDING / SPONSORING ORGANIZATION		8b. OFFICE SYMBOL (if applicable)	9. PROCUREMENT INSTRUMENT IDENTIFICATION NUMBER		
8c. ADDRESS (City, State, and ZIP Code)		10. SOURCE OF FUNDING NUMBERS			
		PROGRAM ELEMENT NO.	PROJECT NO.	TASK NO.	WORK UNIT ACCESSION NO.
11. TITLE (Include Security Classification) RETROREFLECTANCE OF WIRES AND CABLES AT 10.6 MICROMETERS (U)					
12. PERSONAL AUTHOR(S) Mark Savan and Dallas N. Barr					
13a. TYPE OF REPORT Final		13b. TIME COVERED FROM Aug 87 TO Dec 87		14. DATE OF REPORT (Year, Month, Day) January 1988	15. PAGE COUNT 30
16. SUPPLEMENTARY NOTATION					
17. COSATI CODES			18. SUBJECT TERMS (Continue on reverse if necessary and identify by block number)		
FIELD	GROUP	SUB-GROUP	Wire Reflectance: Laser Radar, Carbon Dioxide Lasers		
19. ABSTRACT (Continue on reverse if necessary and identify by block number)					
Quantitative measurements of reflectance are made for a variety of field wires using an infrared laser operating at 10.6 micrometers. Results are presented as plots of retroreflectance versus viewing angle for stranded metallic, insulated, and weathered wires and cables in wet and dry states. Performance implications are discussed for a possible wire avoidance system. Retroreflectance is found to be greatly decreased for the wet wires. For the case of 6mm diameter copper wire the reduction of retroreflectance at normal incidence of approximately 15 dB results in a decrease of detection range from 3.6 to 1.8km for a typical wire detection system. Weathered wires are shown to have a much more diffuse retroreflectance distribution. For the 6mm copper wire, retroreflectance of the weathered sample is lower than that of the unweathered by 10 dB at normal incidence, but is higher by 10 dB at 50 degrees. This results in a decrease of detection range from 3.7 to 2.4km at normal incidence and an increase from 1.3 to 2.0km at 50 degrees.					
20. DISTRIBUTION / AVAILABILITY OF ABSTRACT <input checked="" type="checkbox"/> UNCLASSIFIED/UNLIMITED <input type="checkbox"/> SAME AS RPT <input type="checkbox"/> DTIC USERS			21. ABSTRACT SECURITY CLASSIFICATION Unclassified		
22a. NAME OF RESPONSIBLE INDIVIDUAL Mark Savan		22b. TELEPHONE (Include Area Code) 703 / 664-4931		22c. OFFICE SYMBOL AMSEL-RD-NV-L	

PREFACE

Wires and other obstacles of small, cross-sectional areas have been significant safety hazards to low-flying Army helicopters for many years. With the increased use of nap-of-the-earth and terrain contour flight techniques, the probability of wire strikes occurring increases. Also, substantial increases in the cost of the newer, more sophisticated Army helicopters such as the Apache (AH-64) make the economic impact of associated equipment losses more critical, even without considering losses of highly trained and valued personnel. During fiscal years 1981 through 1983, Army records showed that 20 wire strikes occurred, resulting in 13 fatalities and \$12 million in equipment losses.

The Army needs a low-cost, lightweight sensor which is capable of providing helicopter pilots sufficient warning of the existence and location of wires to allow evasive action. Laser radar is the strongest candidate technology for this application because of the high angular and range resolution it can provide consistent with volume and weight constraints. Coherent carbon dioxide laser radar operating at a wavelength of 10.6 micrometers is one of the options under consideration for this purpose.

In order to adequately model and predict performance of candidate sensor designs, quantitative retroreflectance information on types and conditions of wires and cables expected to be encountered in the field is needed. Measurements of wire retroreflectance at 10.6 micrometers have been reported previously by several authors.^{1,2} The investigation reported herein extends the data base to include other wires and, more importantly, measures the retroreflectance when the wires are wet and after weathering has occurred. As will be shown in this report, the latter two cases are significantly worse than dry, unweathered wires since reflectance is substantially reduced under those conditions. System performance implications are considered and detection range is related to retroreflectance for a variety of conditions.



Accession For	
NTIS GRA&I	<input checked="" type="checkbox"/>
DTIC TAB	<input type="checkbox"/>
Unannounced	<input type="checkbox"/>
Justification	
By	
Distribution/	
Availability Codes	
Dist	Avail and/or Special
A-1	

TABLE OF CONTENTS

Section	Page
I Wire and Cable Retroreflectance Measurements.....	1
Experimental Configurations.....	1
Retroreflectance Distributions.....	2
Measurement Procedures.....	4
II Results and Discussion.....	8
III Conclusions.....	18
Wire Retroreflectance.....	18
System Performance Implications.....	18
Future Plans.....	20
Footnotes.....	24

Figures

1	Optical Configuration Used for Measurements.....	1
2	Geometric Configuration for Monostatic System.....	4
3	Flowers of Sulfur (Cosine Corrected).....	6
4	Relative Size of Test Wires Compared to Laser Beam.....	7
5	Solid Aluminum Wire Comparison.....	9
6	Stranded Copper Wire (4mm).....	10
7	Stranded Copper Wire (6mm).....	11
8	Stranded Copper Wire (10mm).....	12
9	Stranded Aluminum Wire (10mm).....	13
10	Insulated Aluminum Wire (10mm).....	14
11	Army Communications Wire.....	15
12	Weathered Copper Wire (4mm).....	16
13	Weathered Copper Wire (6mm).....	17
14	Range Performance of Wire Detectors (Bare Aluminum Stranded Wire (10mm)).....	21
15	Range Performance of Wire Detectors (Insulated Wire (10mm)).....	22
16	Range Performance of Wire Detectors (Bare Copper Stranded Wire (6mm)).....	23

SECTION I. WIRE AND CABLE RETROREFLECTANCE MEASUREMENTS

Experimental Configurations

The optical configuration is shown in Figure 1. The detection scheme is offset homodyne. Bragg cells are used to create a frequency difference of 10.7 MHz between the local oscillator and transmit beams. A portion of the transmitted radiation is reflected back to the system by the wire sample and is mixed with the local oscillator. The transmit and receive apertures are displaced from each other by a distance of approximately 3 cm. This results in an angular displacement of less than 1° as seen from the sample. The sizes of the transmit and receive apertures are determined by the beam waist at the laser output mirror and by an adjustable iris placed in front of the detector. The iris was adjusted to a diameter of approximately 3 mm, making it the same size as the beam waist. We will thus assume that the two apertures are one and the same; i.e., the system is effectively monostatic.

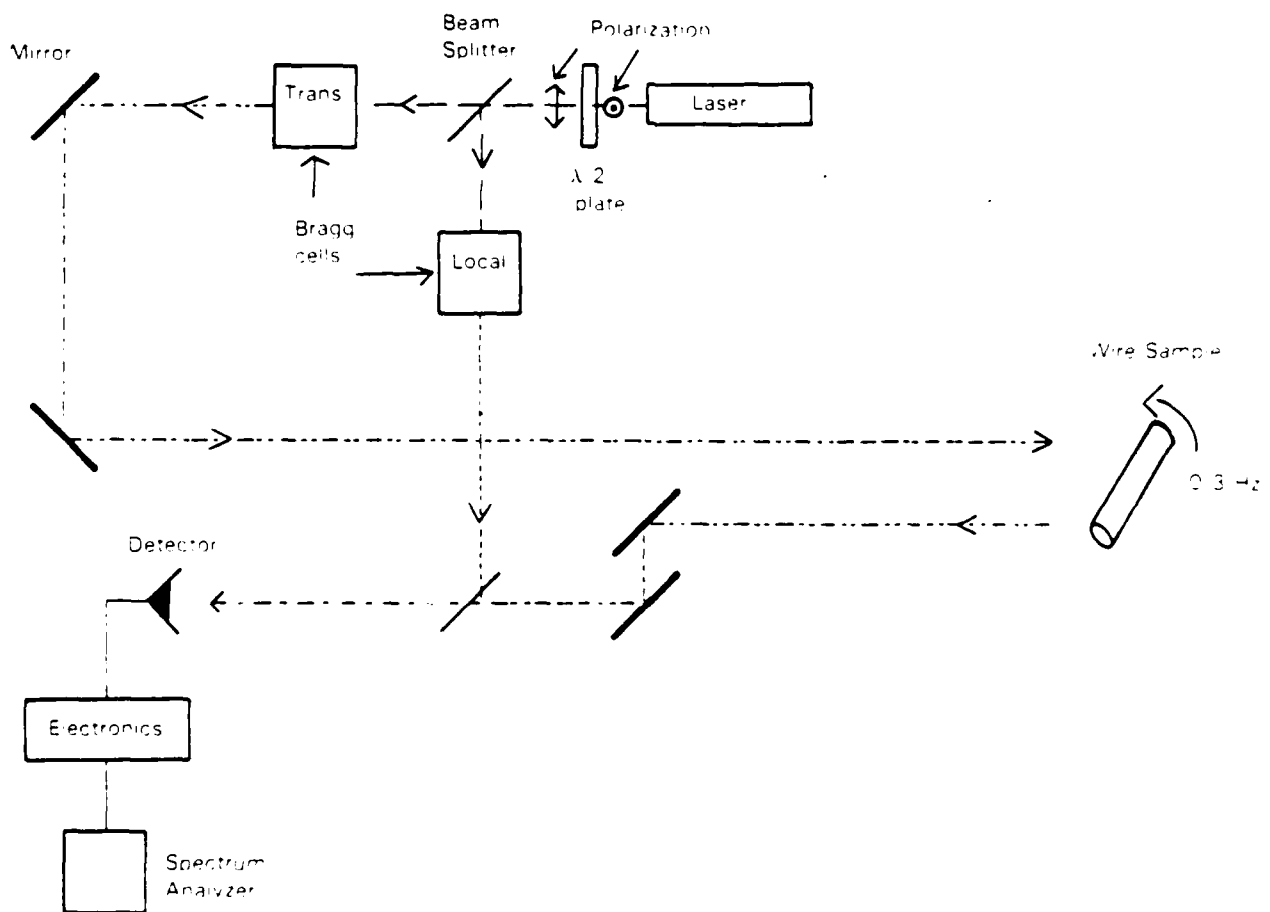


Figure 1. Optical Configuration Used for Measurements

The signal is electronically processed through a bandwidth of 30 KHz and the detector voltage, which is proportional to the return signal, is measured with a spectrum analyzer. The wire sample is placed at a distance of 6 meters from the transmit aperture, and is oriented parallel to the optical table. The incident radiation is polarized horizontally. Speckle and glint averaging is accomplished by rotating the wire about its long axis at a constant rate of approximately 0.3 Hz. This results in a maximum frequency shifting of the return signal on the order of 1 KHz which lies well within the system bandwidth. For the wet measurements, wires were wetted by irrigating the above samples. Copper tubing was positioned above the wires and water was delivered through a series of holes in the tubing.

Retroreflectance Distributions

The retroreflectance, f , is defined by:

$$d\Phi_r = f \Phi_i d\Omega_r \quad [1]$$

so that

$$f = \frac{d\Phi_r}{\Phi_i d\Omega_r} \quad [2]$$

- Ω_r = Solid angle subtended by the receive aperture
- Φ_i = Incident flux
- Φ_r = Reflected flux

This retroreflectance can be equated to the bidirectional reflectance distribution function by noting that the former is just a special case of the latter when the transmit and receive aperture are the same size and located in the same position. In other words, retroreflectance is the monostatic equivalent of bidirectional reflectance.

The comparison of two reflecting samples allows us to write the ratio of the retroreflectances as:

$$\frac{f_1}{f_2} = \frac{\frac{d\Phi_{r,1}}{\Phi_{i,1} d\Omega_{r,1}}}{\frac{d\Phi_{r,2}}{\Phi_{i,2} d\Omega_{r,2}}} \quad [3]$$

Assuming that the two samples have identical geometries, and that the radiation incident on them from the laser radar is constant, we have for the monostatic case:

$$\frac{f_1}{f_2} = \frac{d\Phi_{r,1}}{d\Phi_{r,2}} \quad [4]$$

In this experiment, sample 1 is the wire to be measured and sample 2 is a reference standard. The retroreflectance for the wire sample is given by:

$$f_1 = f_2 \frac{d\Phi_{r,1}}{d\Phi_{r,2}} \quad [5]$$

The transfer standards for this experiment were strips of sandpaper cut to the same width of the wire to be tested. Sandpaper samples have been shown to be excellent approximations to Lambertian surfaces in previous experiments³ as well as by using this apparatus.

The reflectivity, ρ , of a material is defined as the ratio of the total reflected power in all directions to the incident power.⁴ Using a Lambertian reflector and integrating the cosine distribution of reflected power over the hemisphere into which power is reflected, it can be shown that the relationship between reflectivity and reflectance is:

$$f = \frac{\rho}{\pi} \quad [6]$$

Combining equations [5] and [6] gives:

$$f_1 = \frac{\rho_2}{\pi} \frac{d\Phi_{r,1}}{d\Phi_{r,2}} \quad [7]$$

For the case of heterodyne detection:¹

$$d\Phi = K \frac{V^2}{A}$$

K = Constant

V = Detector output voltage

A = Detector area

[8]

Substituting this result into equation [7] gives the result for the retroreflectance of the wire sample:

$$f_1(\theta) = \frac{\rho_2}{\pi} \frac{V_1^2}{V_2^2} \quad [9]$$

Measurement Procedures

The experiment consisted of measurements of reflectance for the monostatic case which is shown in Figure 2. Three major types of wires were studied: stranded metallic, consisting of aluminum and copper wires; insulated; and weathered metallic wires, of all which were measured in both wet and dry states. Descriptions of the individual samples are given in Table 1. The procedure was verified by measurements on a 4 inch diameter disc of flowers of sulfur. This sample has been shown previously^{3,5} to be an excellent approximation to a Lambertian, or perfectly diffuse, reflector at this wavelength. The reflectivity has been measured to be between 0.5 and 0.8 for such a surface. For a Lambertian reflector, the reflectance falls off as the cosine of the incident angle. Plotted in Figure 3 is the retroreflectance of the sulfur. The values are divided by the cosine factor, so that the surface should plot as a straight line. It is seen that the results are very much as expected. The sharp peak at normal incidence is an irregularity of this particular sample, and has been observed in previous experiments. Converting the retroreflectance values to reflectivity and integrating over the possible viewing angles, we obtain a reflectivity value of 0.85 which is near the range of previously obtained values.

In order to simulate an actual wire detection system and avoid scaling errors due to the position of the wire in the beam, it is essential that the beam be larger than any of the samples. The relative sizes of the samples as compared to the laser spot are depicted in Figure 4. The portion of the beam not irradiating the sample can be reflected by background objects causing spurious signals. To eliminate this, the beam is directed by a gold mirror onto a disc of rotating black felt. The felt itself has a reflectance of 4.7% and is rotated at a rate of 78 Hz. The beam is incident at approximately 4 inches from the center of the disc at an angle of approximately 60° so that the background signal is shifted in frequency by 66 Hz and lies outside the processing bandwidth.

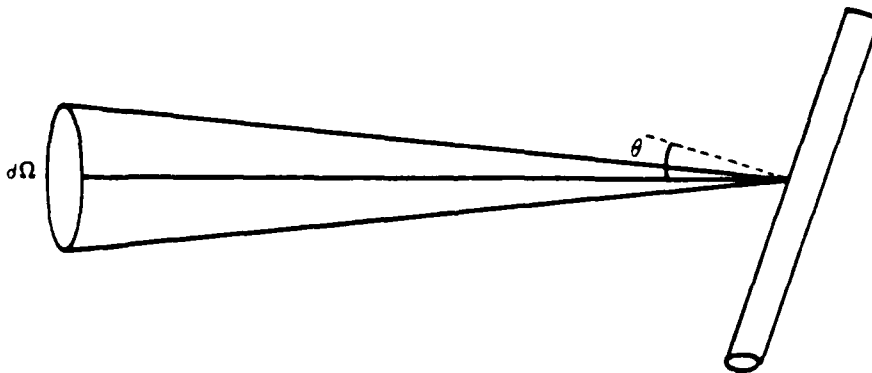


Figure 2. Geometric Configuration for Monostatic System

Table 1. Wires and Cables Measured

METALLIC

Aluminum	10 mm	Six strands in helical arrangement about center strand.
Copper	4 mm	Six strands in helical arrangement about center strand.
Copper	6 mm	Six strands in helical arrangement about center strand
Copper	10 mm	Twelve strands in helical arrangement; center is made of the 4 mm sample described above.

INSULATED

Aluminum	10 mm	Strand arrangement as above; enclosed in black insulation.
Army communication		Insulated pair, 1.7 mm each in side-by-side arrangement.

WEATHERED

Copper	4 mm	Surface tarnished and corroded uniformly over all surfaces.
Copper	6 mm	Surface tarnished on all surfaces. Corrosion present between strands.

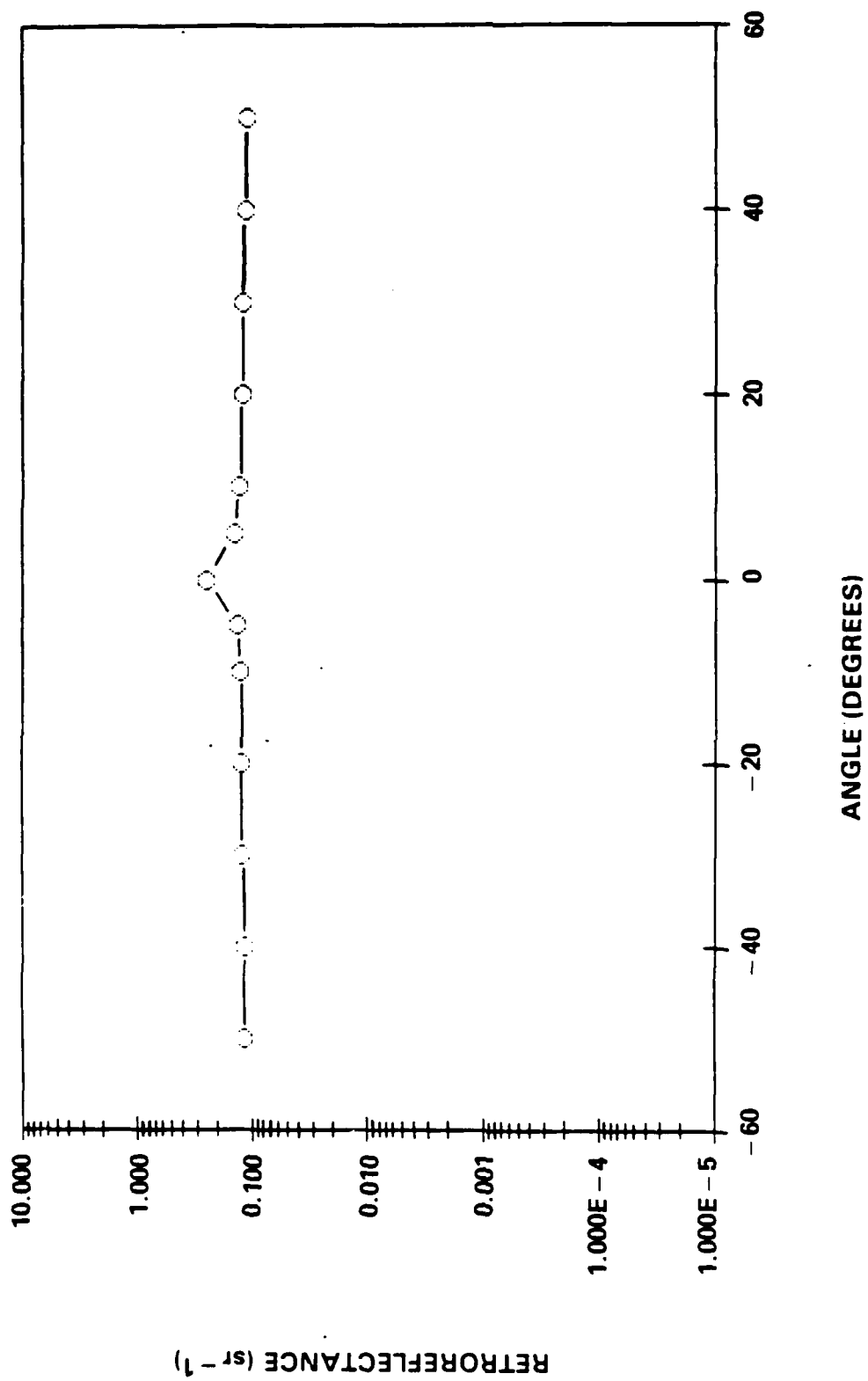


Figure 3. Flowers of Sulfur (Cosine Corrected)

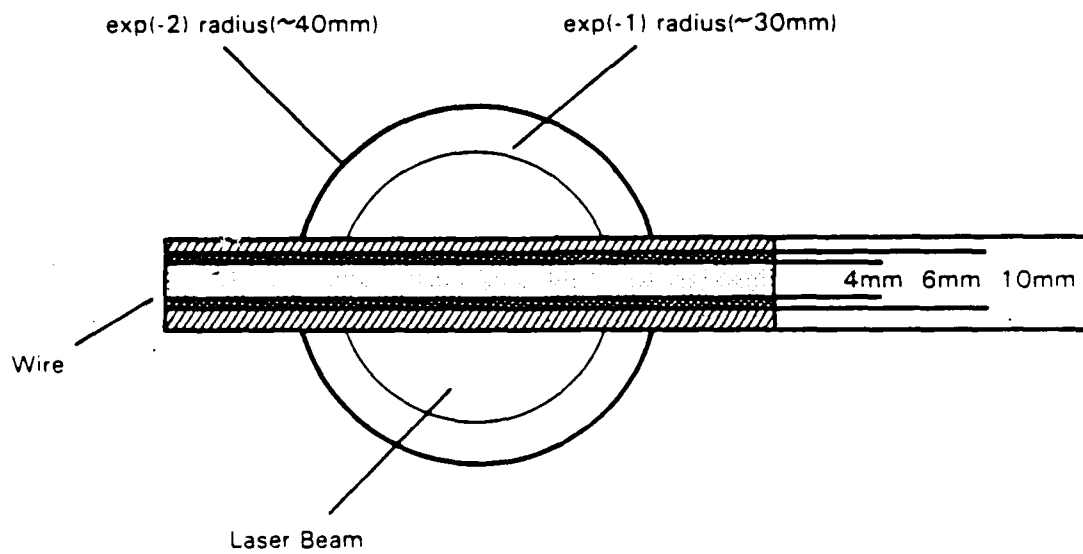


Figure 4. Relative Size of Test Wires Compared to Laser Beam

SECTION II. RESULTS AND DISCUSSION

Solid aluminum wire was measured for the purpose of comparison with the work by Hayes and Brandewie.¹ Their paper presents results as reflection coefficients. Dividing these values by π converts them to retroreflectance values. Figure 5 shows a comparison between the results of the two experiments expressed in terms of the retroreflectance. Again, close agreement exists.

The distributions of the stranded, non-insulated wires (Figures 6 through 9) had central peaks with width of approximately 20° at full width, half maximum. This central structure consisted of two outer peaks located at approximately 10° on either side of normal. Between these two positions, the retroreflectance dipped slightly at and near normal incidence. The stranded wires consist of 7 to 19 strands wrapped in a helical arrangement. For a typical wire of 10 mm diameter, one strand wraps completely around the cable through a length of 180 mm corresponding to a strand pitch of 10° . When the cable is viewed from an angle of approximately 10° on either side of normal, the strands at the very top or bottom of the wire, which are inclined at 10° with respect to the face of the wire, will be reflecting the laser beam normally thus causing a peak in the retroreflectance. The height of these peaks is determined by the specularity of the wire surface. The peak-to-valley ratio, defined here as the ratio of the retroreflectance at normal incidence to that at 20° , was in the range of 100 for the stranded cables with the copper wires having larger values than the aluminum.

The cables took on a drastically different appearance when wet. The most significant change was a 1 or 2 order of magnitude drop in retroreflectance for normal incidence. The peaks at $\pm 10^\circ$ disappeared as the retroreflectance assumed a more specular appearance.

The insulated samples (Figures 10 and 11) were much more diffuse. There was a reduction of 2 orders of magnitude in the normal retroreflectance as compared to the non-weathered stranded wires. Peak-to-valley ratios for insulated samples were near 10.

When wet, these samples also became specular. Again, there was a reduction of normal retroreflectance although it was less than 1 order of magnitude. The Army communication wire showed the smallest change when wet, with its normal retroreflectance decreasing by a factor of only 4.

A dramatic change was observed for the weathered samples (Figures 12 and 13). These appeared very diffuse, almost Lambertian in nature. There was a reduction of two orders of magnitude in retroreflectance from the non-weathered samples.

Al-Khatib also measured stranded metallic wires.² Details necessary to make quantitative comparisons of data such as surface composition and condition are not known. In comparing the data presented here with that in Al-Khatib's paper, one finds close agreement with both the measured data and the theoretical predictions of the earlier work.

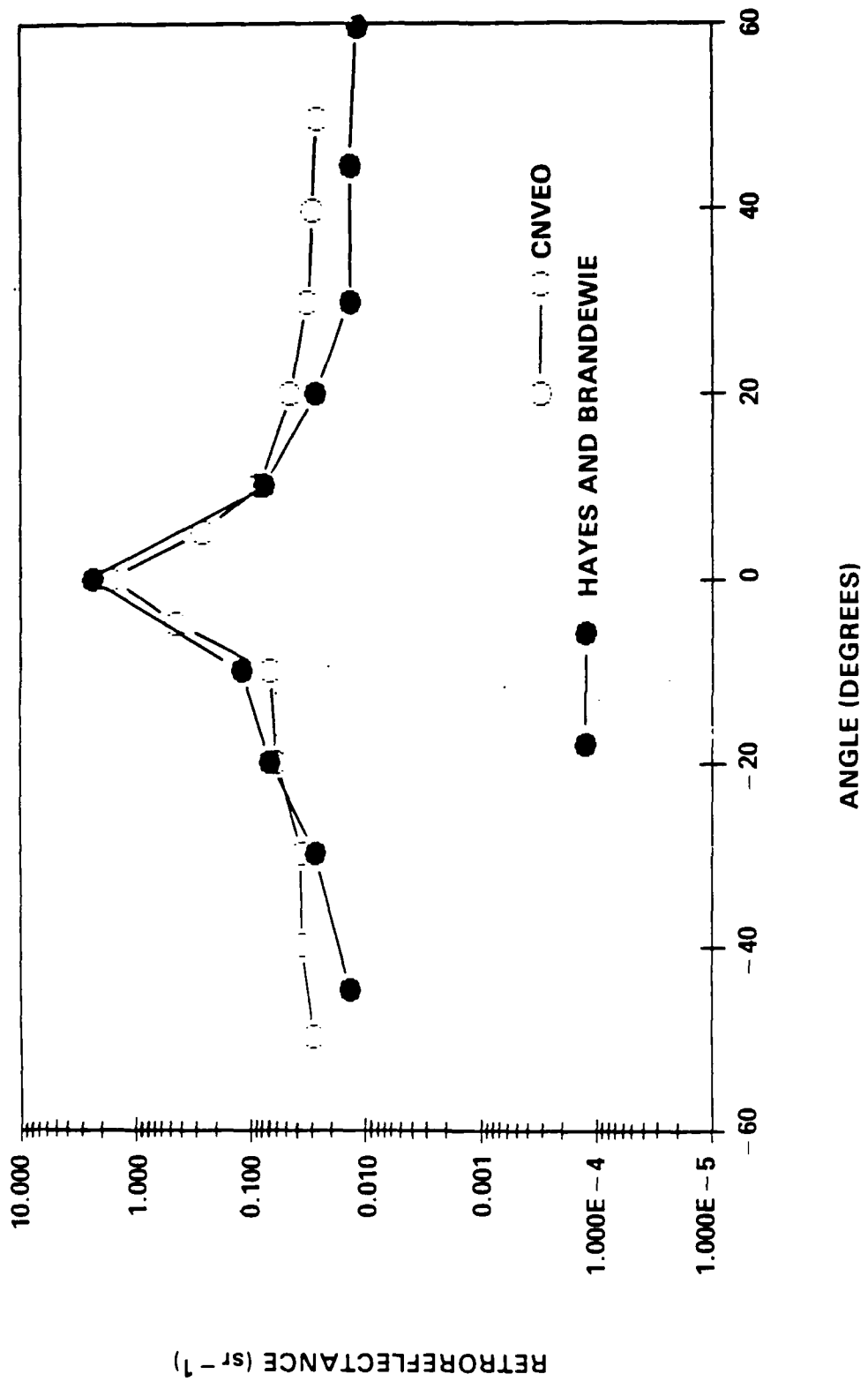


Figure 5. Solid Aluminum Wire Comparison

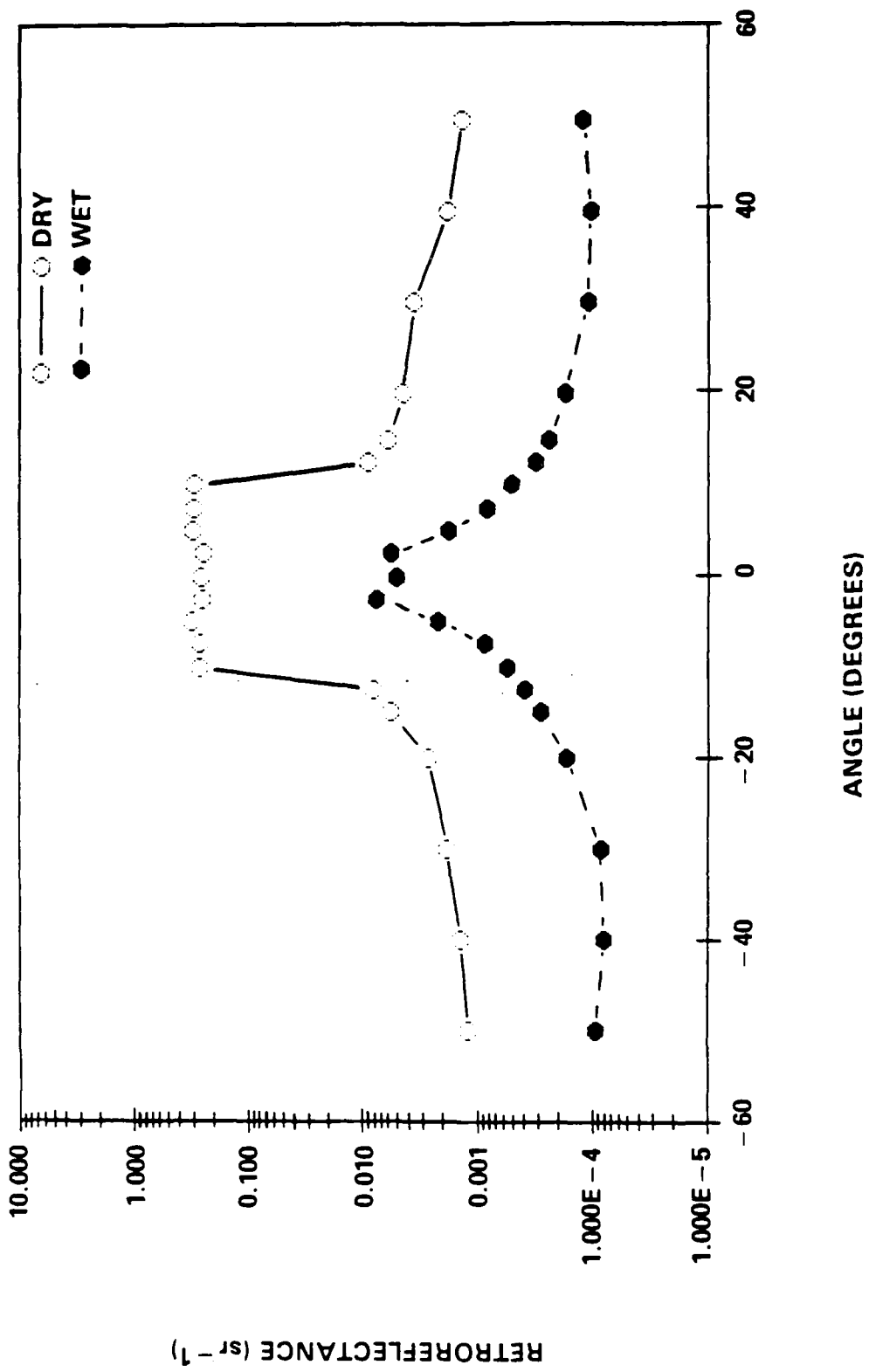


Figure 6. Stranded Copper Wire (4mm)

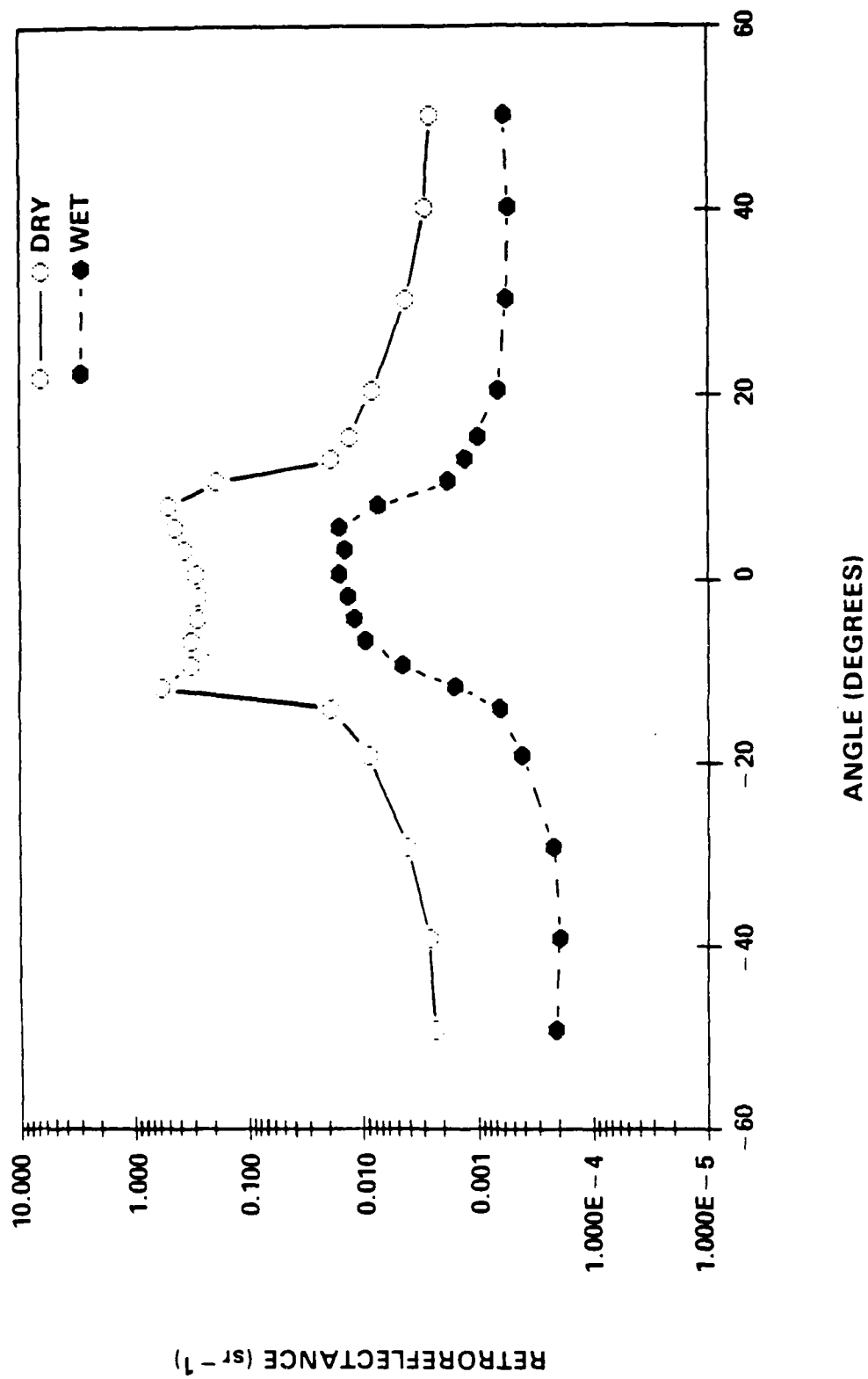


Figure 7. Stranded Copper Wire (6mm)

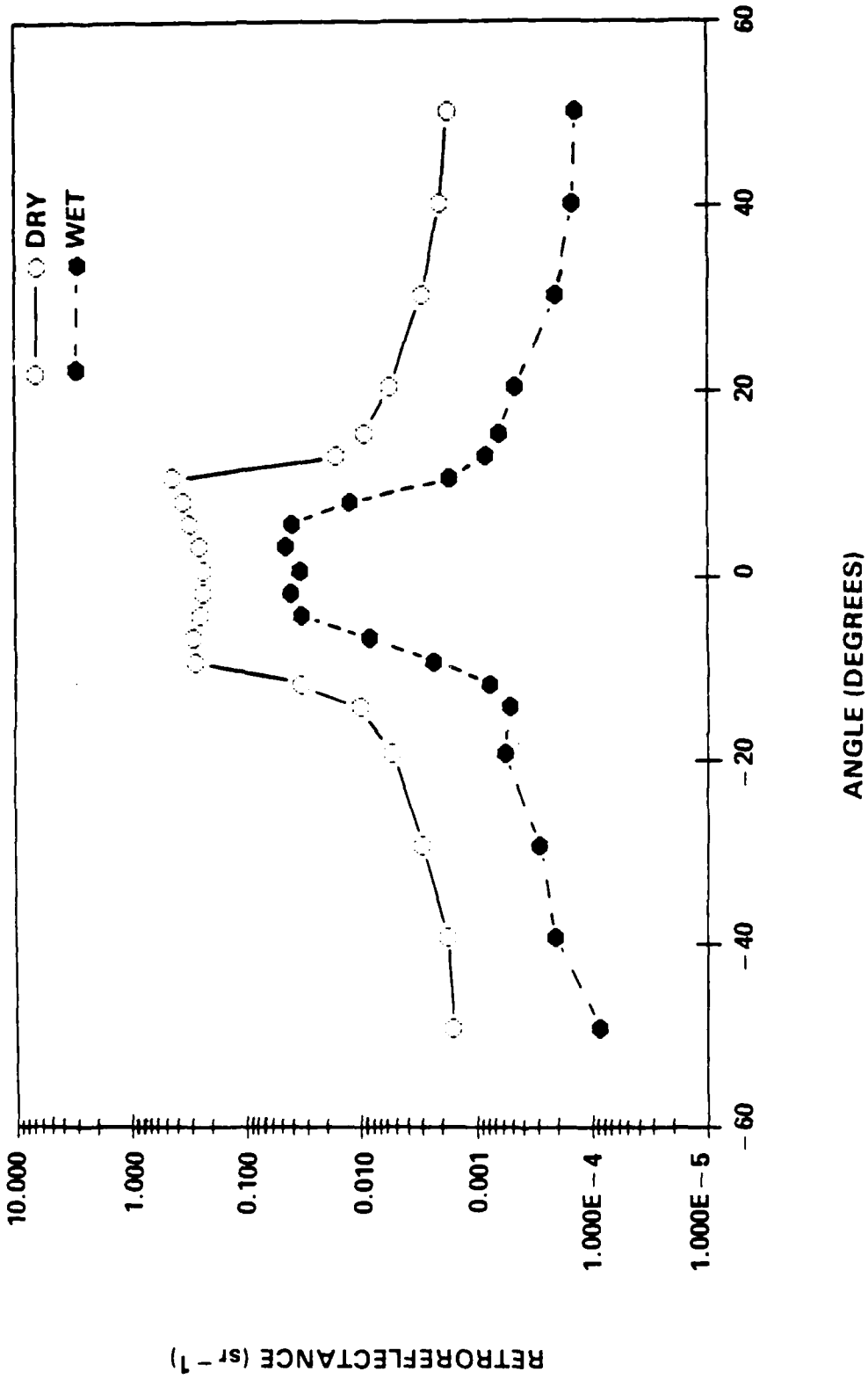


Figure 8. Stranded Copper Wire (10mm)

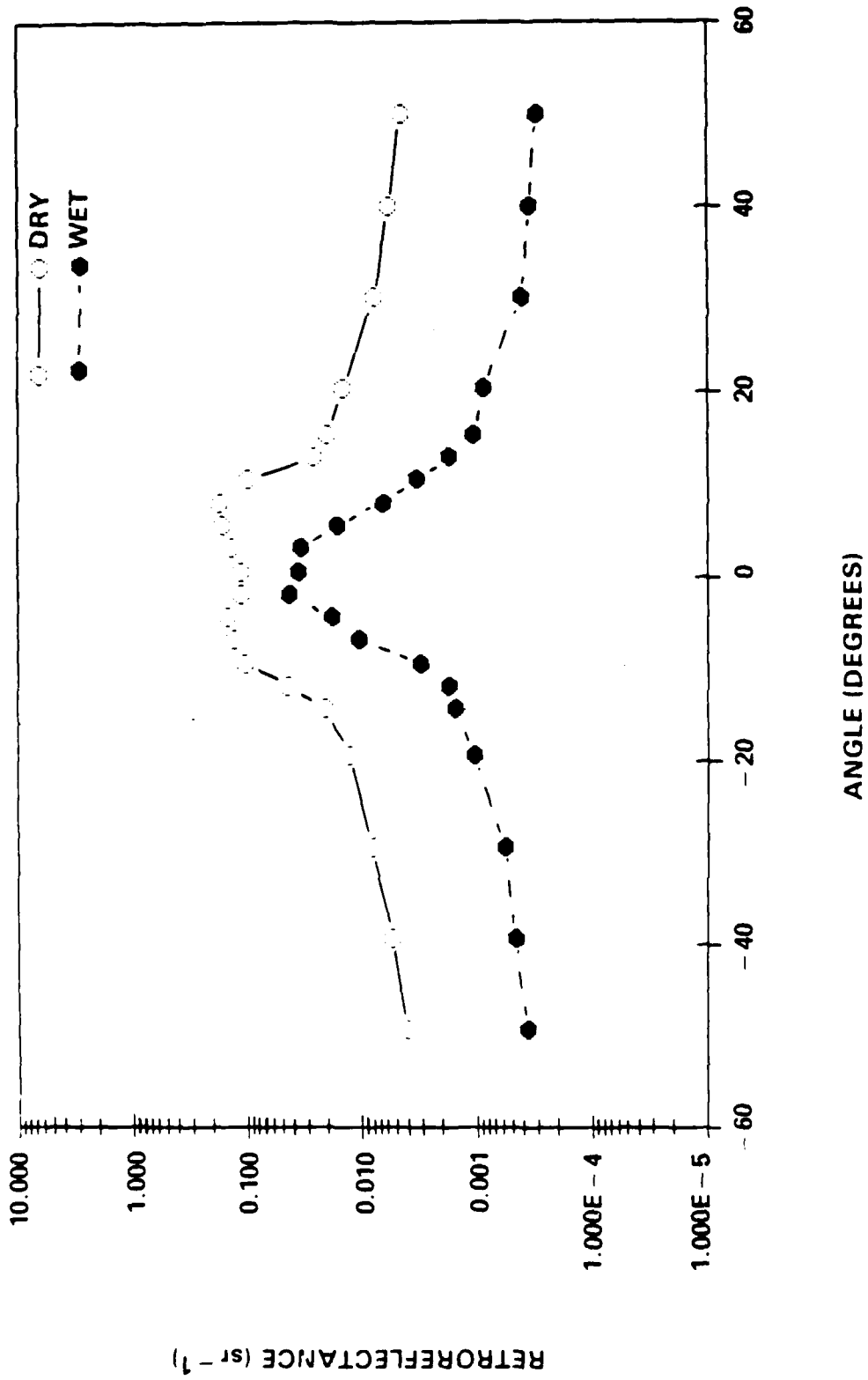


Figure 9. Stranded Aluminum Wire (10mm)

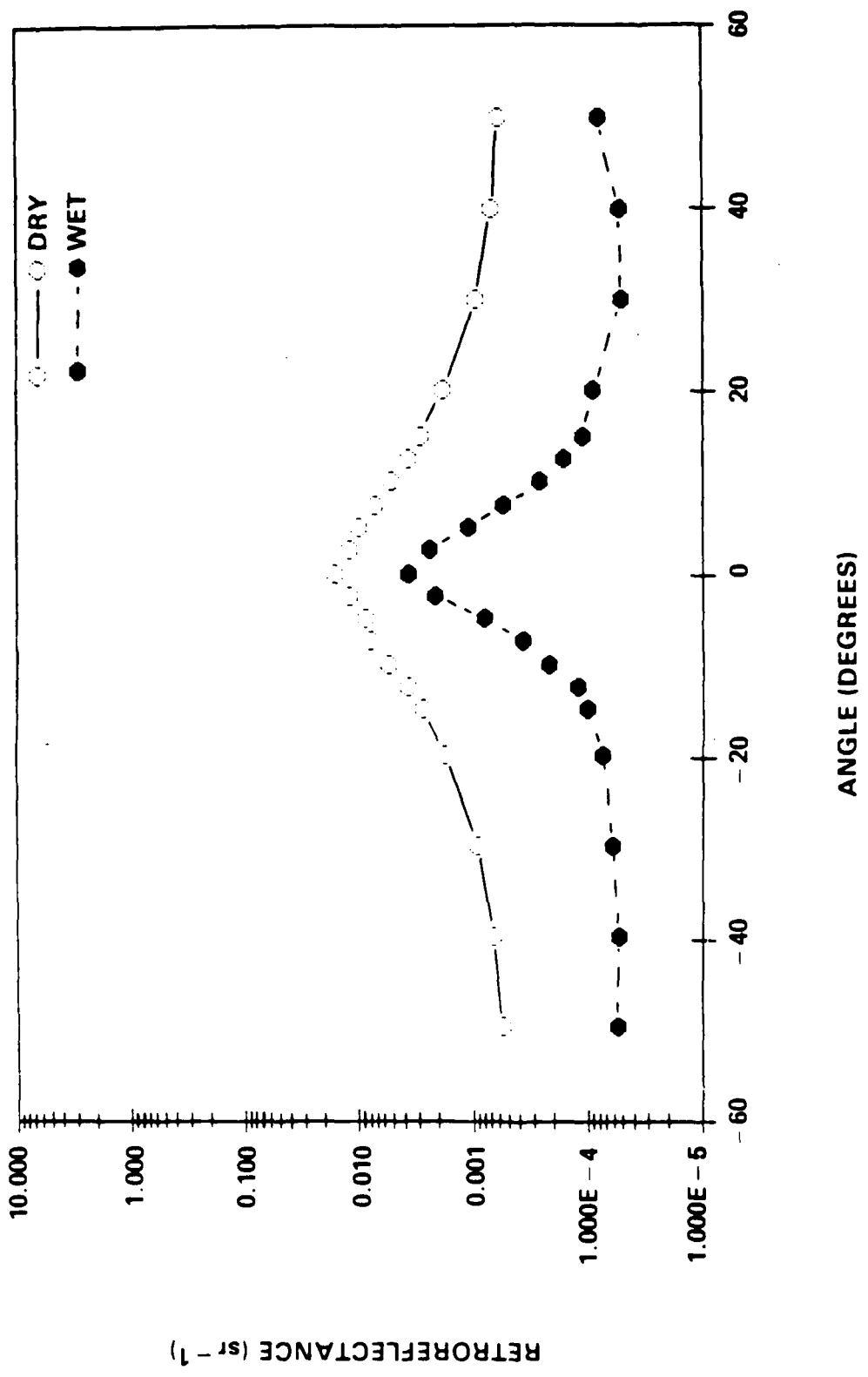


Figure 10. Insulated Aluminum Wire (10mm)

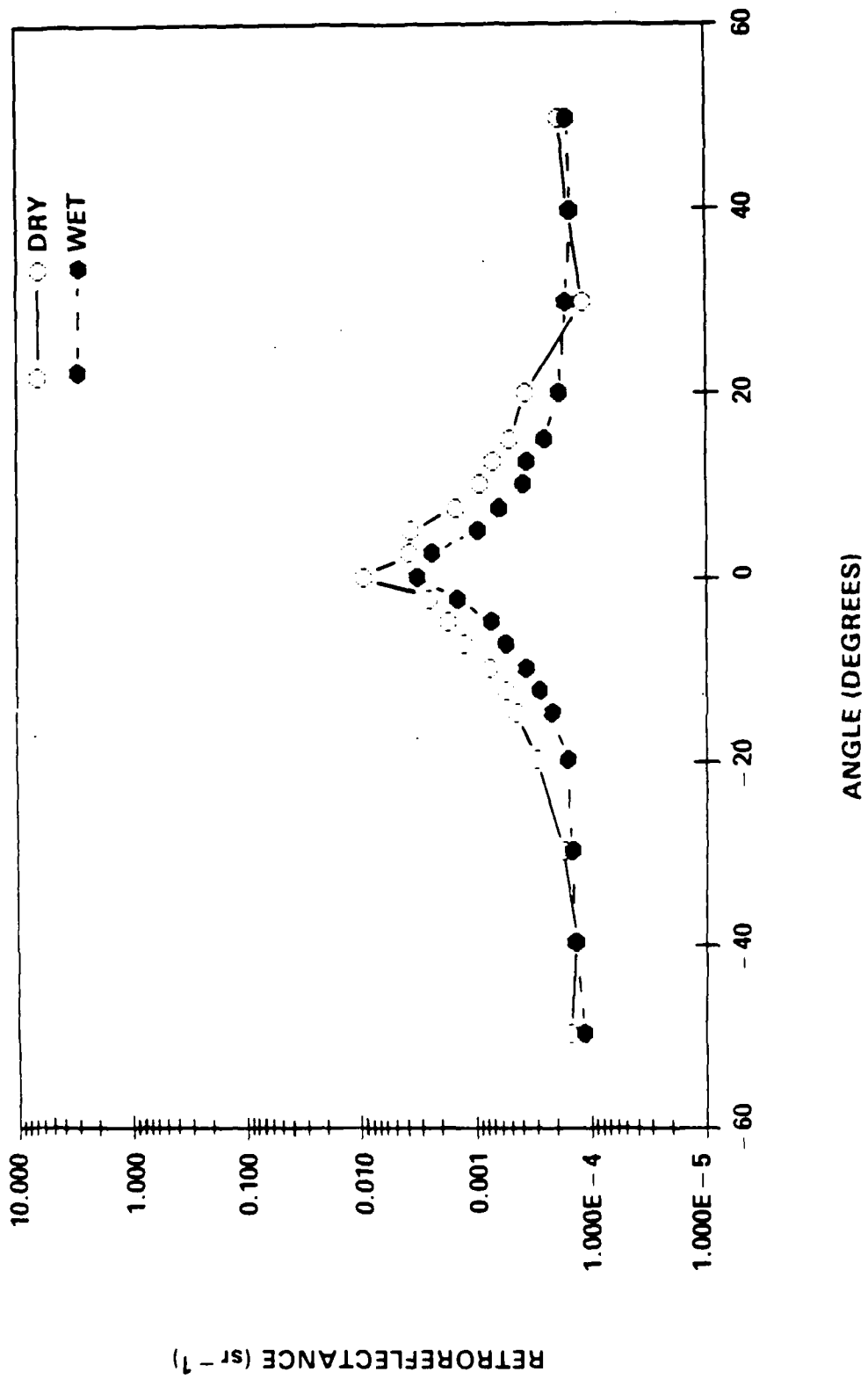


Figure 11. Army Communications Wire

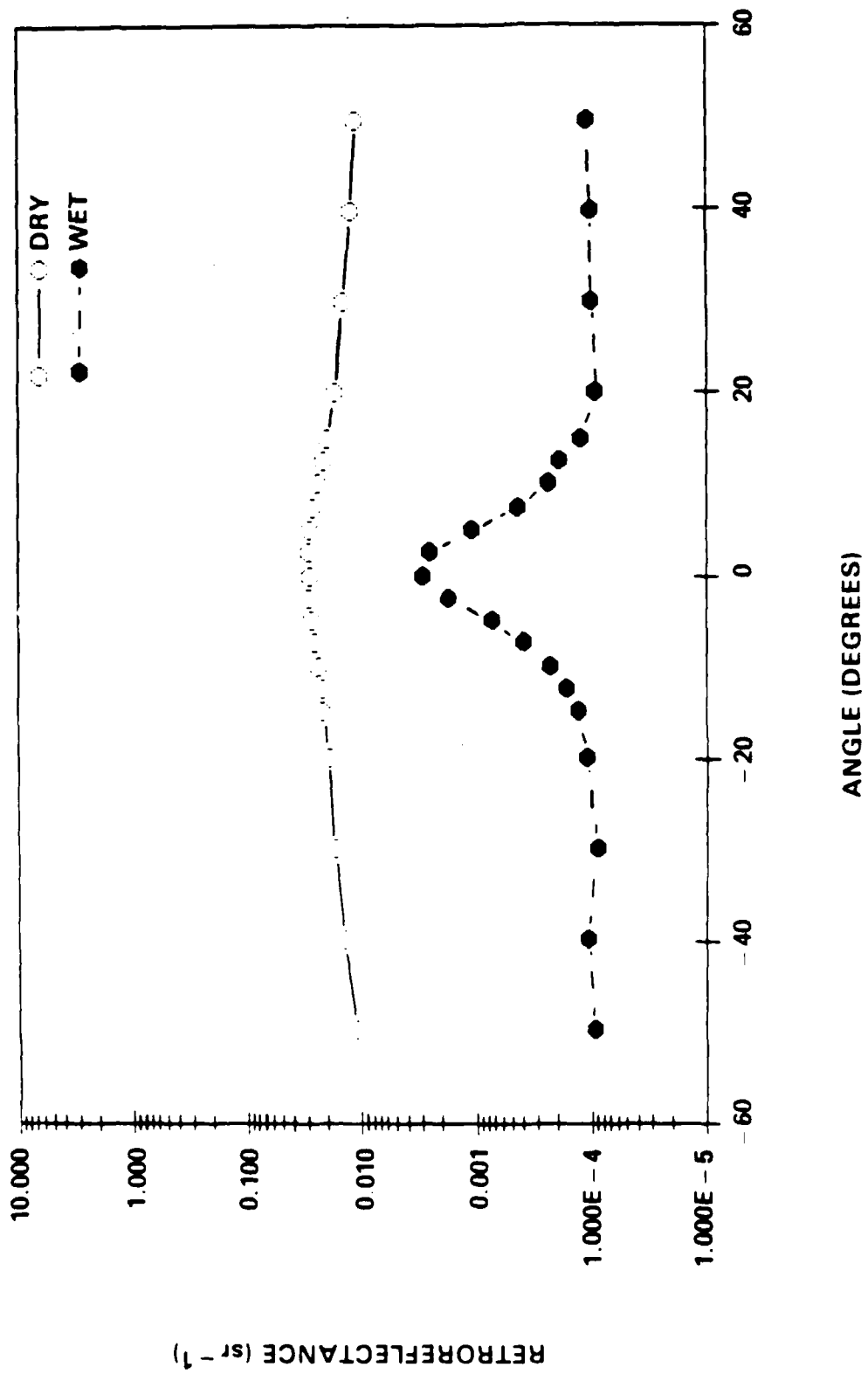


Figure 12. Weathered Copper Wire (4mm)

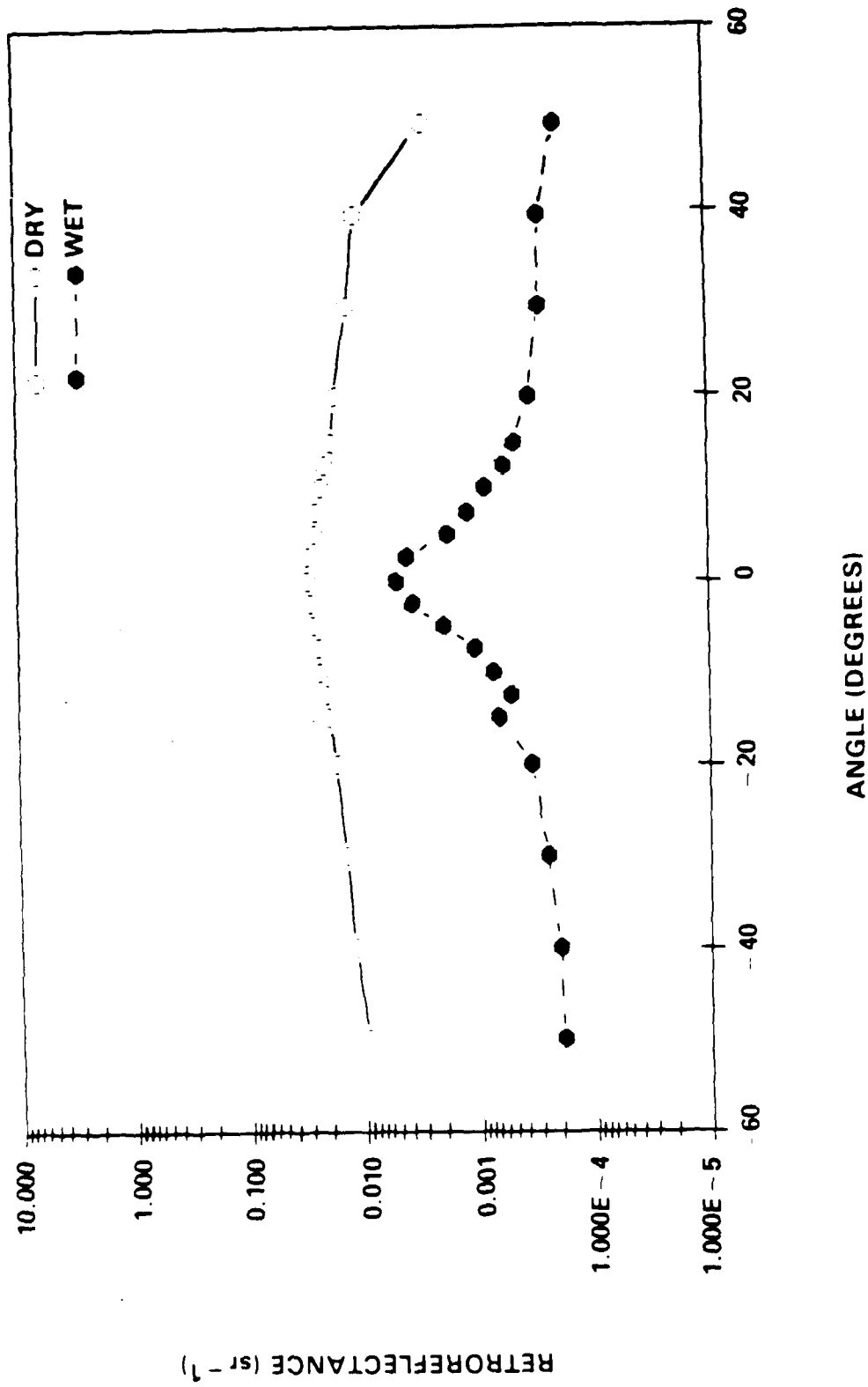


Figure 13. Weathered Copper Wire (6mm)

SECTION III. CONCLUSIONS

Wire Retroreflectance

Within each of the three groups of samples, all of the cables had very similar retroreflectances. There was no significant dependence on the overall size of the cable nor the size or number of individual strands comprising it.

The metallic samples all had fairly broad, tall peaks. Copper samples had slightly higher values than the aluminum, but both showed the very narrow peaks on each side of normal incidence. Reductions of retroreflectance in the range of 1 to 2 orders of magnitude were seen when the wires were wet.

All of the samples looked similar in the wet state, although the metallic samples tended to have slightly broader central peaks. In devising a procedure to irrigate the samples, it was found that the stranded metallic samples, particularly the aluminum, shed water very rapidly. In order to maintain the cables in a completely wet state, it would have been necessary to use an excessive rate of water flow that would have simulated an unnatural environment condition. The result was seen in the broadening of the central peak for the wet data from these samples.

System Performance Implications

The signal-to-noise ratio of a laser radar is determined by:⁴

$$\frac{S}{N} = \frac{P_t A_t A_r \rho' e^{-2\alpha R} \eta}{\Omega_B R^4 h \nu B} \quad [10]$$

where:

- P_t = transmitted power
- A_t = area of the target
- A_r = area of the receiver
- ρ' = target reflectance (ster⁻¹)
- α = atmospheric absorption coefficient
- R = range to the target
- η = overall sensor efficiency
- Ω_B = solid angle of the transmitted beam
- h = Planck's constant
- ν = the optical frequency
- B = the detection bandwidth

For the case of a wire whose diameter (d) is much smaller than the beam but whose length is much larger than the beam,

$$A_t = \pi R^2$$

The other terms are:

$$\Omega_B = \frac{\pi}{4} (\theta_b)^2 = \frac{\pi}{4} \left(\frac{2\lambda}{D_t} \right)^2 \quad [12]$$

$$A_r = \frac{\pi}{4 D_t^2} \quad [13]$$

where D_t is the diameter of the matched transmit and receive aperture, and θ_b is the beam divergence. Substituting these terms into the equation above, we obtain:

$$\frac{S}{N} = \frac{P_t d D_t^2 \rho'(\theta) e^{-2\alpha R} \eta}{2 \lambda R^3 h \nu B} \quad [14]$$

Some further simplification is possible if pulsed modulation is used to measure the range to the wires. We note that:

$$E_p = P_t / B \quad [15]$$

and

$$E_p = P_{ave} / F_r \quad [16]$$

where E_p is the pulse energy, P_{ave} is the average power, and F_r is the pulse repetition frequency. Making these substitutions using $\nu = c/\lambda$ (where c = the speed of light), we have the final signal-to-noise ratio equation:

$$\frac{S}{N} = \frac{P_t d D_t^2 \rho'(\theta) e^{-2\alpha R} \eta}{2 R^3 F_r h c} \quad [17]$$

Using this equation, the signal-to-noise ratio is plotted versus range for several cases of wet and dry wire reflectance at both the normal aspect angle and at 50° off normal. The system parameters assumed are:

$$\begin{aligned} P_{ave} &= 2 \text{ watts} \\ D_t &= 5 \text{ cm} \\ d &= 1 \text{ cm} \\ \alpha &= 1.4 \text{ km}^{-1} \text{ (95 }^\circ\text{F 100}\sigma\text{ relative humidity)} \\ \eta &= 0.1 \\ F_r &= 100,000 \text{ Hz (ambiguous range of 1.5 km).} \end{aligned}$$

The families of curves in Figures 14, 15, and 16 show the range performance under the conditions indicated. The horizontal line suggests a threshold which must be exceeded for acceptable performance. The threshold level of 26.5 dB corresponds to a Rayleigh fluctuating target, one pulse integration, 0.95 probability of detection and 10^{-10} probability of false alarm.⁶ (For a sensor with the pulse repetition frequency assumed above and a 50 nsec pulse width, this will lead to about one false alarm every 17 minutes.) We observe that even under these severe conditions the range performance can be acceptable. Detailed studies of flight profiles and required detection ranges are beyond the scope of this report.

Future Plans

It is planned that similar measurements at wavelengths of both 1.06 and 1.54 micrometers will be made in early 1988. More detailed performance modelling of candidate laser sensors will also be performed.

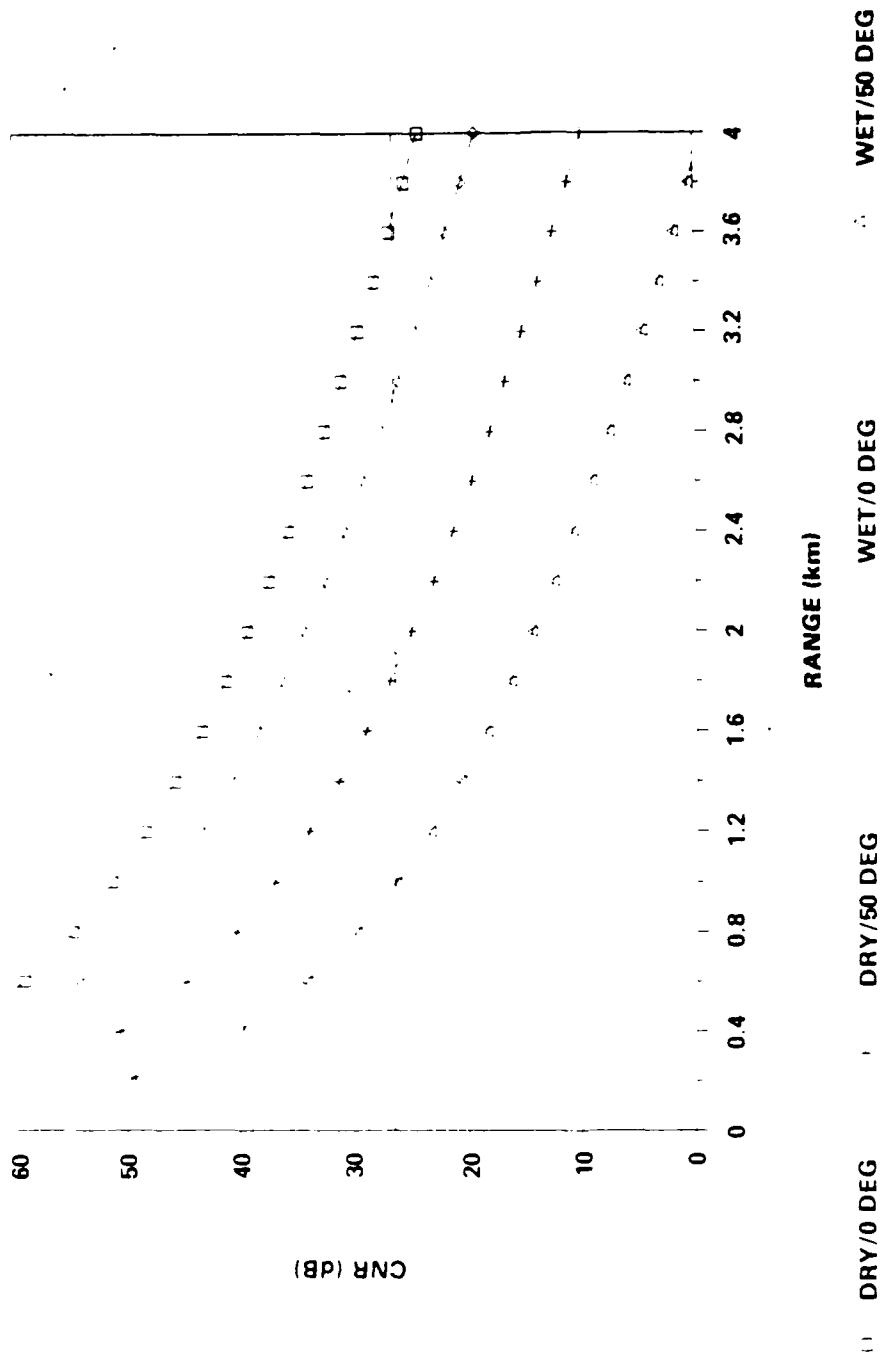


Figure 14. Range Performance of Wire Detectors
(Bare Aluminum Stranded Wire (10mm))

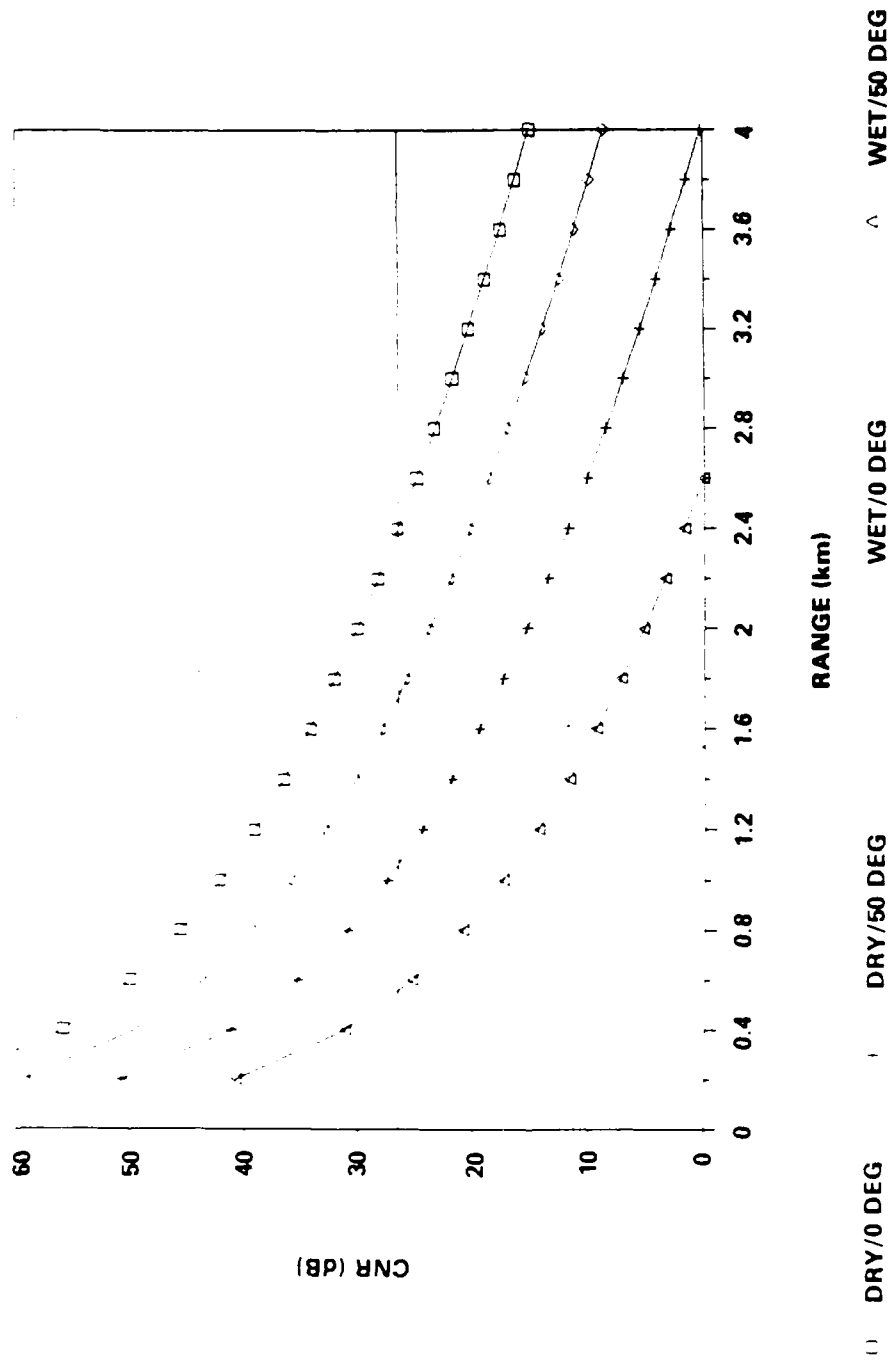


Figure 15. Range Performance of Wire Detectors
(Insulated Wire (10mm))

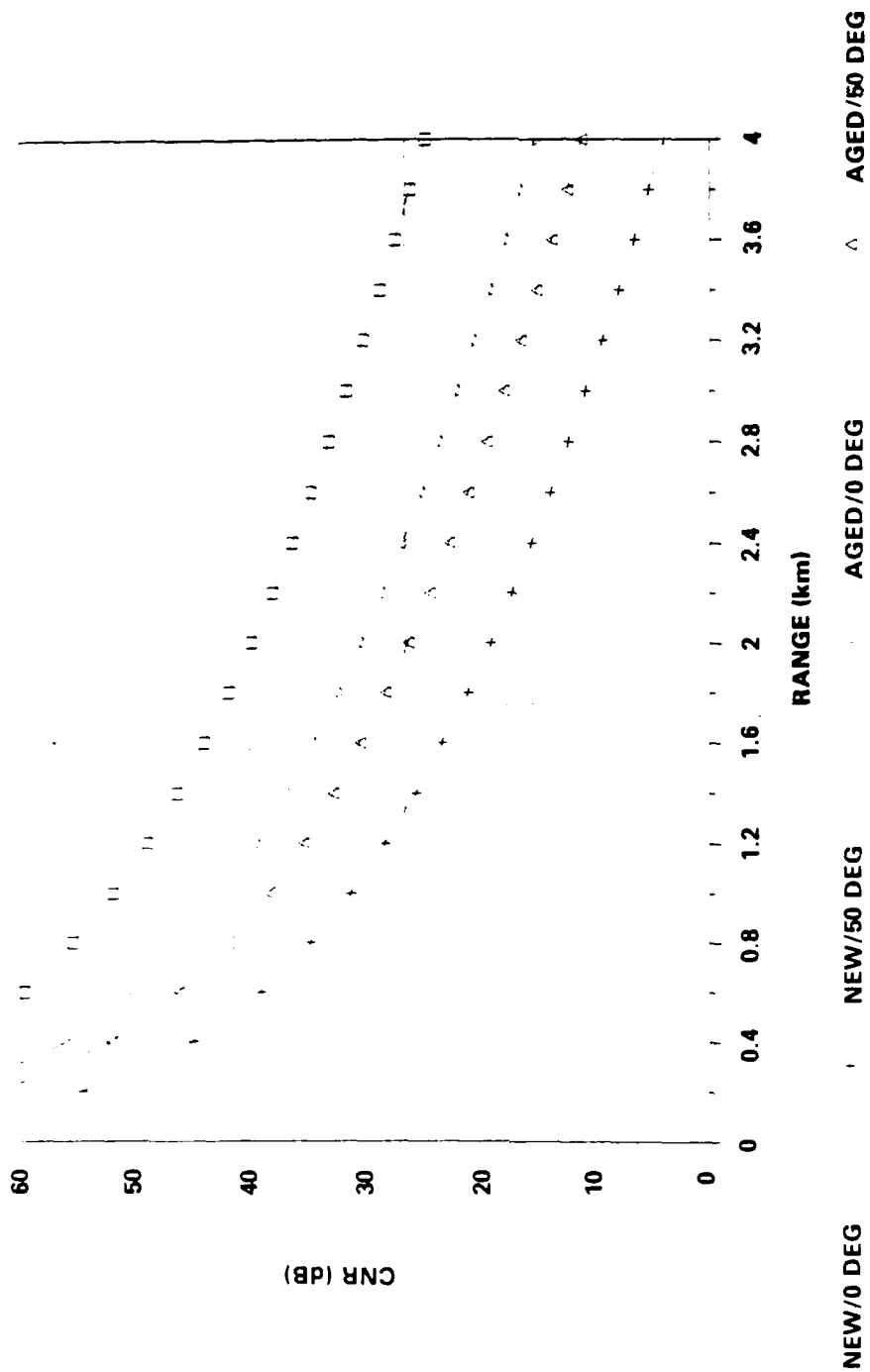


Figure 16. Range Performance of Wire Detectors (Bare Copper Stranded Wire (6mm))

FOOTNOTES

1. C. L. Hayes and R. A. Brandewie, "Reflection Coefficients for Wires and Cable at 10.6 μm ," *Applied Optics* 12(7), July 1973.
2. H. H. Al-Khatib, "Laser and Millimeter-Wave Backscatter of Transmission Cables," *SPIE* v. 300, 1981.
3. T. W. Stuhlinger, E. L. Dereniak, and F. O. Bartell, "Bidirectional Reflectance Distribution Function of Gold-Plated Sandpaper," *Applied Optics* 20(15), August 1981.
4. W. Wolfe and G. Zissis, *The Infrared Handbook*, Office of Naval Research, Department of the Navy (Washington, DC: 1978), pp 1-30.
5. M. Kronstein and R. Kraushaar, "Sulfur as a Standard of Reflectance in the Infrared," *Journal of the Optical Society of America*, 53(4), April 1962.
6. *Radar Handbook*, ed. M. Skolnik (New York: McGraw-Hill, 1970).

DISTRIBUTION FOR REPORT NO. 0063

- | | | | |
|---|--|----|--|
| 1 | Commander
US Army Missile Command
ATTN: AMCPM-RD
Redstone Arsenal, AL 35809 | 1 | Commander
Harry Diamond Lab
ATTN: SLCHD-AC
Adelphi, MD 20783 |
| 1 | Director
Defense Advanced Research Projects
Agency
1400 Wilson Blvd.
Rosslyn, VA 22209 | | CNVEO |
| 2 | Defense Technical Information Center
ATTN: DTIC-FDA
Cameron Station, Bldg 5
Alexandria, VA 22314-6145 | 1 | AMSEL-TMS/SEMCO |
| 1 | Commander
USAAVNC
Ft. Rucker, AL 36362 | 20 | AMSEL-RD-NV-L |
| 1 | Director
Center for Signal Warfare
ATTN: AMSEL-RD-SW-D
Vint Hill Station, VA 22186 | 1 | AMSEL-RD-NV-D
Fort Belvoir, VA 22060-5677 |
| | Project Manager | 1 | Commander
US Army Electronics R&D Command
ATTN: DELSD-L
Ft. Monmouth, NJ 07703-5301 |
| 1 | XM-1 Tank System | 1 | Commander
US Army Communication and Electronic
Command
ATTN: AMSEL-ME-PSL
Ft. Monmouth, NJ 07703-5007 |
| 1 | MICV | | Air Force Wright Aeronautical Laboratories |
| 1 | M60 Tank System
Warren, MI 48090-500 | 1 | ATTN: AFWAL/AARI-1 (Mr. Gerald Shroyer) |
| 1 | Project Manager
TOW DRAGON
Redstone Arsenal, AL 35809 | 1 | AFWA/AADO
Wright Patterson AFB, OH 45433 |
| 1 | Project Manager
TDAS/PNVS
ATTN: AMCPM-AAH-TP
St. Louis, MO 63166 | 1 | Naval Weapons Center
ATTN: Mr. Robert Hintz
Code 31506
China Lake, CA 93555 |
| 2 | Commander
Belvoir RD&E Center
ATTN: STRBE-BT
Tech Library
Fort Belvoir, VA 22060-5606 | 1 | Raytheon Company
Equipment Division
Electro-Optics Laboratory
ATTN: Mr. Greg Osche
528 Boston Post Road
Sudbury, MA 01776 |
| 3 | Commander
Belvoir RD&E Center
ATTN: STRBE-BPG
Pictorial Support Division
Fort Belvoir, VA 22060-5606 | 1 | United Technologies Research Center
400 Main Street
ATTN: Dr. B. Silverman
East Hartford, CT 06108 |
| | | 1 | CLS Group Litton Laser Systems
5 Jeffrey Drive
ATTN: Dr. Robert DelBoca
P.O. Box 767
South Windsor, CT 06074 |
| | | 1 | Commander
US Naval Research Lab
Washington, DC 20375 |

END
DATE
FILMED

4-88

DTIC